European Physical Journal Plus, Volume 137, Issue 3, March 2022, Article number 393
DOI:10.1140/epjp/s13360-022-02579-w

HEAT TRANSFER ENHANCEMENT OF MAGNETIZED NANOFLUID FLOW DUE TO A STRETCHABLE ROTATING DISK WITH VARIABLE THERMOPHYSICAL PROPERTIES EFFECTS

Olalekan Adebayo Olayemi[1,2], Adebowale Martins Obalalu[3], Christopher Bode Odetunde[4], Olusegun Adebayo Ajala[5]

[1]School of Engineering, Cranfield University, Cranfield, United Kingdom.

[1]Department of Aeronautics and Astronautics, Kwara State University, Malete, Kwara State, Nigeria.

[3]Department of Physics, Augustine University, Ilara Epe, Lagos State, Nigeria.

[3]Faculty of Engineering, Augustine University, Ilara-Epe, Lagos State, Nigeria.

[5]Department of Pure and Applied Mathematics, Ladoke Akintola University of Technology, Ogbomoso, Nigeria.

*Correspondence: olalekan.a.olayemi@cranfield .ac.uk

ABSTRACT

Ferrofluid is a one-of-a-kind substance that functions both as a magnetic solid and as a liquid. In this article, water-based Fe_3O_4 and Mn-$ZnFe_2O_4$ nanofluids between parallel stretchable spinning discs are considered. To carry out the study, the influence of rotational viscosity in the flow, which is due to the difference in rotation between the fluid and magnetic particles, and the applied magnetic field are examined. Additional impacts incorporated to the novelty of the model are the variable viscosity and variable thermal conductivity. The Legendre-based collocation method (LBCM) is used to solve the set of governing equations. To ensure the code validity, a comparison with analytical results is conducted and an excellent consensus is accomplished. Comparisons of the pertinent parameters on the flow profiles are displayed in tabular and graphical forms. Analyses reveal that the ferromagnetic Fe_3O_4 nanofluid shows higher thermal conductivity strength than the ferromagnetic Mn-$ZnFe_2O_4$ nanoparticles. This study finds its usefulness in aerospace, biotechnology, medical sciences, material sciences, and so on.

KEYWORDS: Ferromagnetic, nanofluids, Legendre-based collocation method, variable viscosity, and variable thermal conductivity.

1. INTRODUCTION

Colloidal liquids are ferrofluids made up of nanoscale ferromagnetic particles (about 10 nanometers in size) suspended in a carrier liquid. Surfactants are applied to the combination of carrier liquid and nanoparticles to avoid particle agglomeration and create a stable magnetic fluid [1]. Ferrofluid behaves like a regular liquid when there is no magnetic field. Meanwhile, the fluid magnetizes in the direction of the Magnetic flux density with the existence of a strong magnetic field. The behavior of ferrofluid under the influence of a magnetic field distinguishes it from the regular fluid. However, in a state of zero-gravity conditions, Ferrofluids have the ability to flow. When it comes to applications, ferrofluids are frequently used as a rotary seal in computer hard drives. Also, Ferrofluids are utilized as a refrigerant to avoid coil heating of loudspeakers [2, 3]. Magnetic fluids are utilized in various applications, including

engineering and medicine [4-6]. One of the most significant uses of ferrofluid is in the diagnosis and treatment of cancer, as well as a rotating shaft for motors.

Figure 1. The spinning shafts inside a hard drive.

Ferrofluids are utilized in hard drives to produce liquid seals around spinning shafts in the presence of a strong magnetic field (see Figure 1). However, to extend the life span of hard disk drives, a tiny quantity of magnetic fluid is put in the space between the rotating shaft and magnet. several researchers have been interested in the problem of ferrofluids within a rotating system due to their industrial applications, e.g., Production of computer disk, rotating machines, and crystallization process. Regarding this, Von Karman pinpointed the infinite rotating disk problem for steady flow by simplifying the Navier-Stokes equations to a set of ordinary differential equations [7]. Also, [8, 9] improved these findings much further by extending the problem to flow that starts abruptly from rest. In addition, the study of rotating ferrofluids might be useful and interesting in the development of ferrofluid applications in the future. Likewise, research to date has focused on conventional viscous fluid flows exposed to rotating disks [10-13]. Non-Newtonian fluids have also been explored in this kind of flow [14-17]. Moreover, studies have also explored MHD flow under the influence of a rotating disk [18-20]; because of the high physical relevance of these kinds of flows, more studies have been conducted to examine nanofluid rotational flow in the presence of different thermofluidic physical parameters [17, 21-23].

A magnetic force can be used to create greater cooling performance, enhanced rate of heat transfer, and thermal conductivity. Magnetic nanofluid technologies are becoming more attractive in industries due to its varied applications such as in gastrointestinal drugs [24], sterilizing devices [25], biomaterials for wound treatment [26], and other related fields. Several studies have shown that magnetic nanofluid solutions containing nanoparticles of the same size as DNA or protein exhibit excellent performance[27, 28]. Magnetic nanoparticle-based bio suspensions have been employed in targeted medication delivery, magnetic resonance imaging (MRI), and asthma treatment [24]. The inference of magnetic field on nanofluid flow due to rotating disk with viscous dissipation was studied by [29]. Uddin et al.[30] utilized the model of bio-nano-materials processing to investigate the impact of applied magnetic field on convective boundary layer flow and observed that the velocity reduces due to rising in Magnetic field parameters. These articles [31-34] show more development of Magnetic nanofluid.

The viscosity of magnetic fluids and flow characteristics play a significant part in the optimization of ferrofluid properties and as such, various computational techniques have been employed to tackle the difficulty of heat transport characteristics and nanofluids in the existence of strong magnetic field and varying thermal conductivity in various rotating channels such as deformable rotating disk, [35, 36], rotating cavities [37, 38], porous disk [39, 40], rotating cavity with radial outflow [41, 42], dual rotating extendable disk [43, 44]. Viscosity and thermal conductivity are very sensitive to temperature rise, which usually results in significant changes in the physical properties of the fluid, most especially in the theory of lubrication, where they are being affected by the heat produced through the internal friction and a corresponding temperature rise. In recent years, the Maxwell model was used by scientists to characterize the variable thermal conductivity and viscosity of liquids [45]. Just the concentration of nanoparticles is taken into account in the Maxwell model. Several researchers are exploring this approach to develop modified models that represent liquid properties [7]. This research complements and builds on other research such as: (i) Magnetoviscous impacts on ferrofluids [46, 47]. (ii) The analysis of heat transfer enhancement in the flow of magnetic fluid [48-50]. (iii) Heat transfer enhancement using various kinds of ferrofluid flows and heat transfer analysis [51]. The process of irreversible thermodynamic is significant in the study of heat transfer, therefore, the heat transport analysis with entropy generation has therefore been considered by the researcher [52, 53]. The heat transport enhancement of various kinds of nanofluids has also been investigated by [4, 39]. The study of heat transfer and convection is essential for nanofluidic engineering applications [54, 55]. In previous research work, the strength of the magnetizing body force was not considered while analyzing the fluid velocity and heat transmission.

The particular concern of the current work is to study the ferrohydrodynamic of water-based Fe_3O_4 and Mn-$ZnFe_2O_4$ nanofluids due to Parallel Stretchable Rotating disks. The implication of magnetization force on flow motion and heat propagation is analyzed. Also, the viscosity due to the applied magnetic field in a Stretchable Rotating Disk is examined in the present study. Moreover, the thermal conductivity of the nanofluid varies with the temperature.

To the best of our knowledge, up until now, no study into these problems has been reported. Additionally, the interaction of thermophysical properties of water and nanoparticles (density, thermal conductivity, and specific heat) inside the magnetized nanofluid flow over a Parallel Stretchable Rotating Disk makes this study more interesting. It is important to point out that cooling of disks using nanofluid is now a major problem in a wide variety of fields. To respond to the current knowledge gap, it is crucial to establish some reasonable models that can supplant the conventional heat transfer model. Magnetized Nanofluids are novel generation material and has received some significance in industrial advancement. The Legendre-based collocation method (LBCM) is used to solve this problem. The thermodynamic properties of the pertinent entrenched fluid dimensionless parameters are investigated on the fluid axial flow rate $f(\eta)$, radial velocity component $f'(\eta)$, tangential dimension $g(\eta)$,and on the temperature distribution

LBCM and their properties are applied to determine the general procedure for solving differential equations with convergence analysis. Thus, LBCM is of great importance to engineers and scientists.

2. MATHEMATICAL MODEL

Figure 2 illustrates the stretchable coaxially rotating disk and its cylindrical coordinates (r, ϕ, z). Magnetization characteristics of Fe_3O_4 and Mn-$ZnFe_2O_4$ are utilized. A magnetic field is applied tangentially and radially. At $z = 0$, the stretchable coaxial disk rotates with uniform angular velocity Ω .The impacts of variable viscosity and variable thermal conductivity are considered when analyzing the heat transfer process. The particles in a magnetic fluid have a different spinning velocity than the flow velocity when a magnetic field is applied. The axial flow rate and fluid temperature for the ferromagnetic fluid are expressed in the following terms [1]

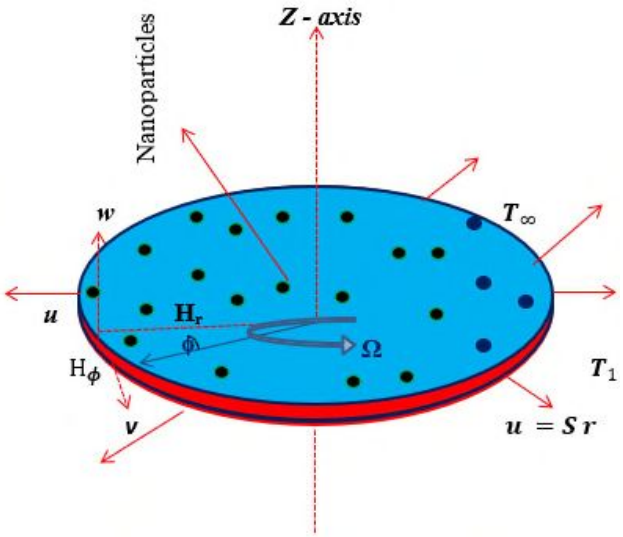

Figure 2:The physical geometry of the flow

$$u_r + w_z + \frac{u}{r} = 0, \tag{1}$$

$$\rho_{nf}\left(u\,u_r + w\,u_z - \frac{v^2}{r}\right) = -p_r - \mu_0 M\,H_r + \mu_{nf}\left\{1 + \frac{3}{2}\phi_1\frac{\delta - \tanh\delta}{\delta + \tanh\delta}\right\}\left(u_{zz} + \frac{1}{r}u_r + u_{rr} - \frac{u}{r^2}\right) - \frac{\mu_{nf}}{k_0}\left\{1 + \frac{3}{2}\phi_1\frac{\delta - \tanh\delta}{\delta + \tanh\delta}\right\}u \tag{2}$$

$$\rho_{nf}\left(u\,v_r + w\,v_z + \frac{uv}{r}\right) = -\mu_0\,\frac{M}{r}H_\phi + \mu_{nf}\left\{1 + \frac{3}{2}\phi_1\frac{\delta - \tanh\delta}{\delta + \tanh\delta}\right\}\left(v_{zz} + \frac{1}{r}v_r + v_{rr} - \frac{v}{r^2}\right) - \frac{\mu_{nf}}{k_0}\left\{1 + \frac{3}{2}\phi_1\frac{\delta - \tanh\delta}{\delta + \tanh\delta}\right\}v \tag{3}$$

$$(\rho c_p)_{nf}(u\,T_r + w\,T_z) = -\mu_0 T\,M_T\left(u\,H_r + \frac{1}{r}v\,H_\phi\right) + \frac{k(T)}{r}\,T_r + (k(T)\,T_r)_r + (k(T)\,T_z)_z + Q_T^*(T - T_c) \tag{4}$$

Subjected to:

$$z = 0\ ; \quad z \to \infty; \quad u = 0,\ u \to 0,\ v = \Omega\, r, \quad v \to 0,\ w = 0, \quad T = T_w\ , T \to T_\infty,\ P = P_\infty \tag{5}$$

The table below displays the description and symbols in the governing equations (1)- (5)

Table 1: Symbols and their descriptions

Symbols	Description	Symbols	Description
f(η),	non-dimensional axial flow rate	(α_{nf})	thermal diffusivity of nanofluid
$f'(\eta)$	dimensionless radial flow rate	Λ	non-dimensional temperature
(Ω)	disk angular velocity	μ_0	permeability of free space
$g\,(\eta\,)$	tangential component flow rate	P(η)	dimensionless pressure
(ρ_{nf})	density of nanofluid	(μ_{nf})	Viscosity of nanofluid
H	intensity of the magnetic field	(S)	disk stretching rate
(T_w)	disk temperature	k(T)	variable thermal conductivity
k(T)	thermal conductivity	k_0	permeability constant
ρc_p	heat capacitance	T_c	Curie temperature
K_1	pyro-magnetic coefficient	D	the vertical distance between disks
T	Temperature	c_p	specific heat
Q_T^*	thermal dependent heat source/sink coefficient	M	magnetization
δ_0	strength of the magnetic field		
θ	non-dimensional axial distance.	$(\beta, \beta_1, \beta_2)$	ferromagnetic interaction number
Pr	Prandtl number	E	variable thermal conductivity

In the presence of a magnetic field, the nanofluid viscosity is described as [7]

$$\mu_{nf}(H \neq 0) = \mu_f\left\{1 + \frac{5}{2}\phi_1\right\}\left(1 + \frac{3}{2}\phi_1\frac{\delta - \tanh\delta}{\delta + \tanh\delta}\right) \tag{6}$$

$$\mu_{nf}\left(1 + \frac{3}{2}\phi_1\frac{\delta - \tanh\delta}{\delta + \tanh\delta}\right) \tag{7}$$

Equation (7) signifies that the strength of the magnetic field depends on viscosity, also the expression in equation (8) vanishes

$$1 + \frac{3}{2}\phi_1\frac{\delta - \tanh\delta}{\delta + \tanh\delta} \tag{8}$$

Temperature-dependent thermal conductivity of nanofluid is defined as [32, 56]

$$k(T) = k_{nf}\left\{1 + \varepsilon\frac{T - T_\infty}{T_w - T_\infty}\right\} \tag{9}$$

In radial and tangential coordinates, the magnetic field modules are defined as follows:

$$H_r = -\frac{\partial \psi}{\partial r}, H_\phi = -\frac{\partial \psi}{\partial \phi}, H_r = \frac{\delta_0}{2\pi}\frac{\cos\phi}{r^2} the\ , H_\phi = \frac{\delta_0}{2\pi}\frac{\sin\phi}{r} \quad (10)$$

The magnetic field intensity is described as [39, 40]

$$H = \sqrt{(H_r)^2 + (H_\phi/r)^2} = \frac{\delta_0}{2\pi\ r^2} \quad (11)$$

The magnetic field intensity rates of radial and tangential components are given as:

$$H_r = -\frac{\delta_0}{\pi\ r^3}, H_\phi = 0 \quad (12)$$

Magnetization is considered a linear function of temperature [51] as:

$$M = K_1(T_c - T) \quad (13)$$

The following definitions [57-59] as presented in Table 2 are utilized in this research.

Table 3 is designed to address the nanomaterials and base thermophysical properties.

Table 2: Thermophysical properties of nanofluid

Property	Nanofluid
Dynamic viscosity	$\mu_{nf} = \frac{\mu_f}{(1-\phi_1)^{5/2}},$
Density	$\rho_{nf} = (1-\phi_1)\rho_f + \phi_1\ \rho_s,$
thermal diffusivity	$\alpha_{nf} = \frac{k_{nf}}{(\rho c_p)_{nf}},$
heat capacity	$(\rho c_p)_{nf} = (1-\phi_1)(\rho c_p)_f + \phi_1\ (\rho c_p)_s,$ $\frac{k_{nf}}{k_f} = \frac{k_s + 2k_f - 2\phi_1()}{k_s + 2k_f + \phi_1(k_f - k_s)}$ $(\rho c_p)_{nf} = (1-\phi_1)(\rho c_p)_f + \phi_1\ (\rho c_p)_s,$ $\frac{k_{nf}}{k_f} = \frac{k_s + 2k_f - 2\phi_1(k_f - k_s)}{k_s + 2k_f + \phi_1(k_f - k_s)}$

Table 3: The physical characteristics of the base fluid and nanoparticles [58]

Physical property	Water(H_20)	Fe_3O_4	Mn-$ZnFe_2O_4$
$\rho/(kg.m^{-3})$	997.1	5200	0.613
$k/(W.mK)$	0.613	1050	6
$C_p/(J.kgK)$	4 179	670	3.9

Introducing the following transformations:

$$\left.\begin{aligned} v = r\ \Omega\ g(\eta),\ p = P_\infty + 2\ \Omega\ \mu_f\ P(\eta),\ \ u = r\ \Omega\ f'(\eta), \\ w = -\sqrt{2\ \Omega v_f}\ f(\eta), T = T_c + (T_w - T_c)\theta(\eta),\ \ \eta = z\sqrt{\frac{2\Omega}{v_f}} \end{aligned}\right\} \quad (14)$$

$$\tau_s = \mu_{nf}\{u_z\}_{z=0}, \tau_w = \mu_{nf}\{v_z\}_{z=0},\ q_w = -(K(T)\ T_z)_{z=0}$$

$$K = \frac{k_0\ \Omega}{v_f}\ ,\quad Pr = \frac{(\rho c_p)_f\ v_f}{k_f}\ , \beta = \frac{\mu_0\ K_a\ \delta_0(T_1 - T_2)}{\pi\ \rho_f\ \Omega^2\ r^4},$$

$$\beta_2 = \frac{\mu_0\ K_a\ \delta_0}{2\ \pi\ r^2(\rho c_p)_f},\ S_T = \frac{Q_T^*}{2\ (\rho c_p)_f\ \Omega},\ \beta_1 = \frac{\mu_0\ K_a\ \delta_0\ T_c}{2\ \pi\ r^2(\rho c_p)_f(T_w - T_c)},$$

$$K_1 = \left\{1 + \frac{3}{2}\phi_1 \frac{\delta - \tanh\delta}{\delta + \tanh\delta}\right\},\quad K_2 = (1-\phi_1)^{2.5},\quad K_3 = \left\{1 - \phi_1 + \phi_1\frac{\rho_s}{\rho_f}\right\},$$

$$K_4 = \left\{\frac{k_s + 2k_f - 2\phi_1\ (k_f - k_s)}{k_s + 2k_f + 2\phi_1\ (k_f - k_s)}\right\},\quad K_5 = \left\{1 - \phi_1 + \phi_1\frac{(\rho c_p)_s}{(\rho c_p)_f}\right\}$$

The transformed equations become:

$$\frac{K_1}{K_2\ K_3}\left(2f''' - \frac{1}{K}f'\right) + (2f\ f'' - (f')^2 + g^2) + \beta\theta = 0 \tag{15}$$

$$\frac{K_1}{K_2\ \ K_3}\left(2g'' - \frac{1}{K}g\right) + 2f\ g' - 2\ f'\ g = 0 \tag{16}$$

$$K_4[(1+\varepsilon\ \theta)\ \theta'' + \varepsilon\ (\theta')^2] + K_5\ Pr\ f\ \theta' - Pr\quad \beta_1\ f' - Pr\quad \beta_2\ f'\ \theta + Pr\quad S_T\ \theta = 0 \tag{17}$$

subjected to:

$$f(0) = 0,\qquad f'(0) = 0,\qquad g(0) = 1,\qquad \theta(0) = 1, \tag{18}$$
$$f'(\infty) = 0,\qquad g(\infty) = 0,\qquad \theta(\infty) = 0$$

The non-dimensional radial stress, tangential stress and Nusselt number for flow are as follows:

$$C_f = \frac{\mu_{nf}}{\rho_f(r\ \Omega)^2}(u_z)_{z=0} \Rightarrow {}^{f\frac{1}{K_2}''}\sqrt{Re} \tag{19}$$

$$C_g = \frac{\mu_{nf}}{\rho_f(r\ \Omega)^2}(v_z)_{z=0} \Rightarrow {}^{g\frac{1}{K_2}'}\sqrt{Re}$$

$$Nu = \frac{q_w}{k_f(T_w - T_c)} \Rightarrow \frac{Nu}{\sqrt{Re}_4{}'}$$

3. A SUMMARY OF LEGENDRE BASED COLLOCATION METHOD (LBCM)

The Legendre-based collocation method (LBCM) is useful in several areas of engineering to solve the numerical solution of (linear, non-linear, fractional) equations. The collocation technique with the Legendre polynomial basis function is used to solve the nonlinear ordinary differential equations (15)-(18) where the solution of closed formed is very similar along with the boundary conditions in equation (18). The problem domain [0; a] is approximated with the domain truncation approach to enforce the proposed method of collocation ([0; L]) where L is the length that must be greater

than the boundary layer thickness. The domain [0; L] must first be transformed into the domain [1;1] on which the Legendary collocation method can be applied using algebraic mapping

3.1. APPLICATION OF LEGENDRE BASED COLLOCATION METHOD (LBCM*)*

To determine the sensitivity of the entrenched terms, a polynomial basis function is defined for the $f(\eta), g(\eta)$ and $\theta(\eta)$.

$$f(\eta) = \sum_{i=0}^{N} a_i T_i\left(\frac{2\eta}{L} - 1\right), \quad g(\eta) = \sum_{i=0}^{N} b_i T_i\left(\frac{2\eta}{L} - 1\right) \text{ and } \theta(\eta). = \sum_{i=0}^{N} c_i T_i\left(\frac{2\eta}{L} - 1\right) \tag{20}$$

Where a_i, b_i, c_i are the constants to be determined and $T_i\left(\frac{2\eta}{L} - 1\right)$ is the shifted Legendre base function from [1;1] to [0; L]. To obtain the values of constants a_i, b_i, c_i, equation (18) is substituted into the boundary conditions in equation (20) to have.

$$\sum_{i=0}^{N} a_i T_i\left(\frac{2\eta}{L} - 1\right)_{\eta=0} = 0, \frac{d}{d\eta}\sum_{i=0}^{N} a_i T_i\left(\frac{2\eta}{L} - 1\right)_{\eta=0} = 0, \sum_{i=0}^{N} b_i T_i\left(\frac{2\eta}{L} - 1\right) = 0 \tag{21}$$

$$\frac{d^2}{d\eta^2}\sum_{i=0}^{N} a_i T_i\left(\frac{2\eta}{L} - 1\right) = 1 \sum_{i=0}^{N} c_i T_i\left(\frac{2\eta}{L} - 1\right) = 1$$

Where N is a secure whole number and a_i, b_i and c_i are constants to be obtained. These equations are reduced approximately to zero as far as possible using the collocation method in a range depending on the considered boundary conditions as follows.

$$\text{For } \delta(\eta - \eta_k) = \begin{cases} 1, & \eta = \eta_j \\ 0, & otherwise, \end{cases} \tag{22}$$

$$\int_0^L R_f \delta(\eta - \eta_j) d\eta = R_f(\eta_j) = 0, \quad for\ j = 1, 2, .. N - 2 \tag{23}$$

$$\int_0^L R_\theta \delta(\eta - \eta_j) d\eta = R_\theta(\eta_j) = 0, \quad for\ j = 1, 2, .. N - 1$$

$$\int_0^L R_\phi \delta(\eta - \eta_j) d\eta = R_\phi(\eta_j) = 0, \quad for\ j = 1, 2, .. N - 1$$

The η_j is defined as the shifted Gause Lobato collocation points. Also, the R_f, R_θ and R_ϕ residuals are integrated over the domain using Simpson's one-third rule due to the difficulty in direct integration to obtain a nonlinear system of equations in a_i, b_i and c_i. The obtained system of equations together with the enacted basis function for the boundary conditions are concurrently solved to determine the unknown a_i, b_i and c_i, which are then substituted in the polynomial basis function to have the required solution.

$$\eta_j = \frac{1}{2}(1 - cos\left(\frac{j\pi}{N}\right)), for j = 0,1 \cdots, N. \tag{24}$$

Finally, the unknown coefficients were computed using MATHEMATICA software. Table 4 shows the LBCM solutions in different Convergence approximation orders. However, the numerical outcomes are in perfect agreement

Table 4. LBCM solutions in different Convergence approximation orders when $\phi_1 = \delta = K = \beta = \beta_1 = \beta_2 = 1, K_1 = 1.0524, Pr = 3, \varepsilon = 0.1$ and $S_T = 1.0$

Number of iteration (N)	$f(\eta)$	$g(\eta)$	$\theta(\eta)$
4	0.449146	0.98388	0.06984
4	0.463215	0.98746	0.06982
6	0.465441	0.180551	0.296789
8	0.465417	0.180558	0.296766
10	0.465417	0.180557	0.296765
12	0.465417	0.180557	0.296766
14	0.465417	0.180557	0.296766
16	0.465417	0.180557	0.296766

4. DISCUSSION

This segment is designed to address the behaviour of the fluid parameters on the fluid axial velocity (f), radial velocity (f'), tangential velocity (g) and temperature (θ) through plots and tables for Fe_3O_4 and Mn-$ZnFe_2O_4$-nanofluids. Unless otherwise stated, the default parameter values are utilized in this study; $\phi_1 = 0.1, \delta = 0.2, K = 0.3, \beta = \beta_1 = \beta_2 = 1, K_1 = 1.0524, Pr = 3, \varepsilon = 0.1$ and $S_T = 1.0$.as default parameters. Figures 2 to 4 show the effect of inverse permeability parameter K on the ferromagnetic Fe_3O_4 and Mn-$ZnFe_2O_4$ Nanofluid flow in a rotating disk. The fluid velocity increases as the rotating disk inverse permeability medium are enhanced such that the fluid viscosity reduces to allow free nanoparticle movement. An increase in the medium's pore stimulates internal heating that resulted in a reduced nanoparticle molecular bonding and decreases nanofluid friction. Thus, the axial, radial and tangential velocities increase all through the flow region.

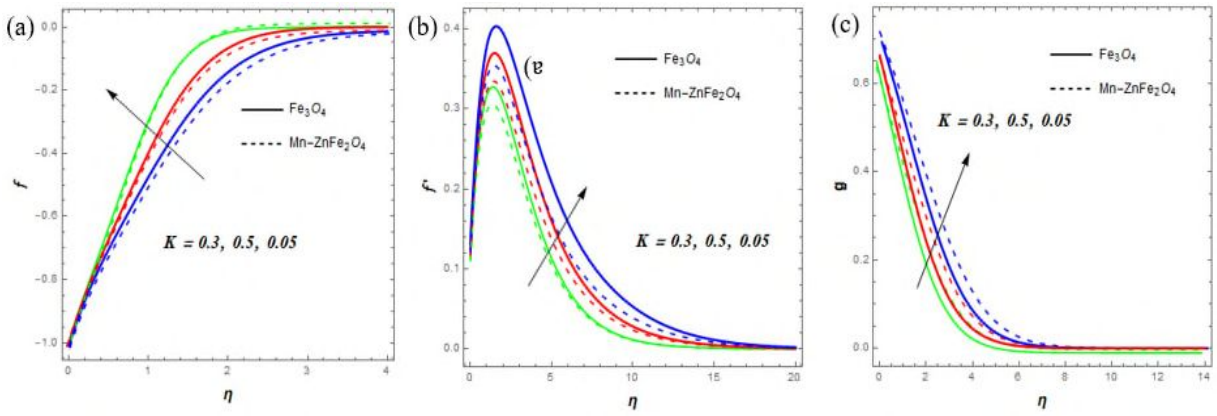

Figure 3: Effects of (K) on (f), (f'), *and* (g) profiles.

The strong magnetic dependence on viscosity is represented by the expression $\mu_{nf}\left\{1+\frac{3}{2}\phi_1\frac{\delta-\tanh\delta}{\delta+\tanh\delta}\right\}$ which emerged in the momentum equations (*2*) and (*3*). The present expression $\frac{3}{2}\phi_1\frac{\delta-\tanh\delta}{\delta+\tanh\delta}$ defuncts in the absence of electromagnetic field because the liquid and nanoparticles rotate at the same angular velocities in the flow. However, the angular motions of the nanoparticles in the flow diverge from the angular velocity of the liquid because of the electromagnetic field effect. Also, this hindrance creates an extra blockage on the fluid in the existence of strong magnetic field, making the magnetic ferrofluid in the flow more viscous. However, the value of δ determines the intensity of the induced magnetic force. Therefore, under the influence of the Lorentz force, the radial motions of the studied Fe_3O_4 and $Mn\text{-}ZnFe_2O_4$ nanofluids reduce, hence, the dynamic viscosity rises due to these effects. Conversely, when the magnetic field strength rises, the tangential velocity (f'), and temperature distribution (θ) improved. Therefore, since the opposing force has a powerful inference on the Lorentz force, hence, the influence of applied magnetic field on the flow behavior is negligible (see Figure 3(b and c).

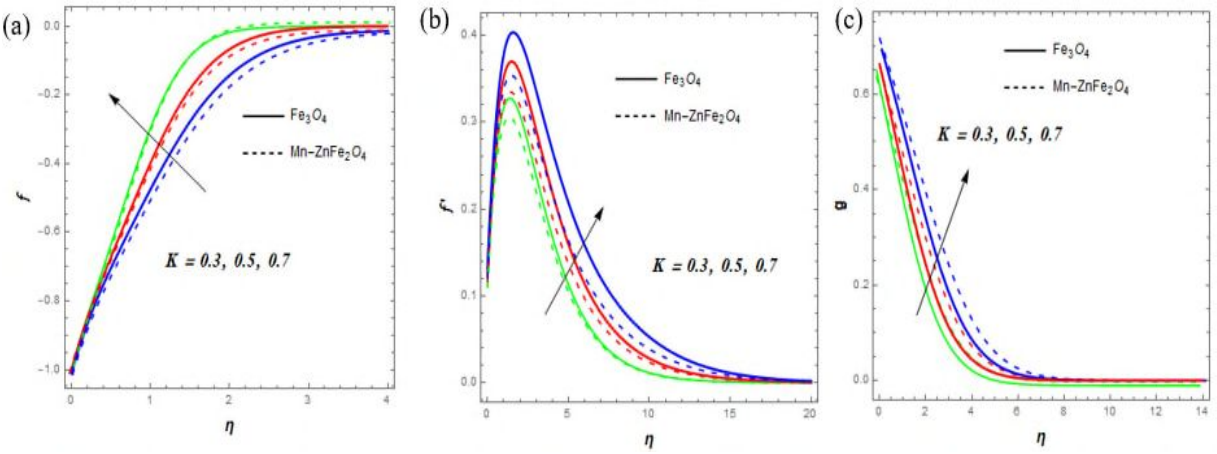

Figure 4:Impacts of (δ) on (f), (f'), *and* (g) profiles.

Figure *6*(a)-(b) displays the distributions of (f), (f'), (g) and (θ) for ferromagnetic interaction number (β). The momentum equation generates this value. However, the breaking of the fluid particle bond enhances the random collision of nanoparticles thereby motivating free flow of the ferromagnetic fluid. Further, the ferromagnetic interaction number (β) has the ability to reverse the speed distribution's direction in the existence of a strong magnetic field. However, at low β values, the flow is directed radially outwards. Also, the flow can direct the center outward in the existence of strong magnetic field. Consequently, due to this characteristic, ferrofluid can be effective in various space applications. Therefore, because of the combined effects of the stretched rotating disk and high intensity magnetic field which increase the viscosity of the liquid and prevent collisions of free nanoparticles, the reduction in temperature distribution signifies that the magnetization force has changed from a thermal force to a vicious force. Therefore, the thermal distribution of the rotating disc profile reduces (see Figure 5(a-d)).

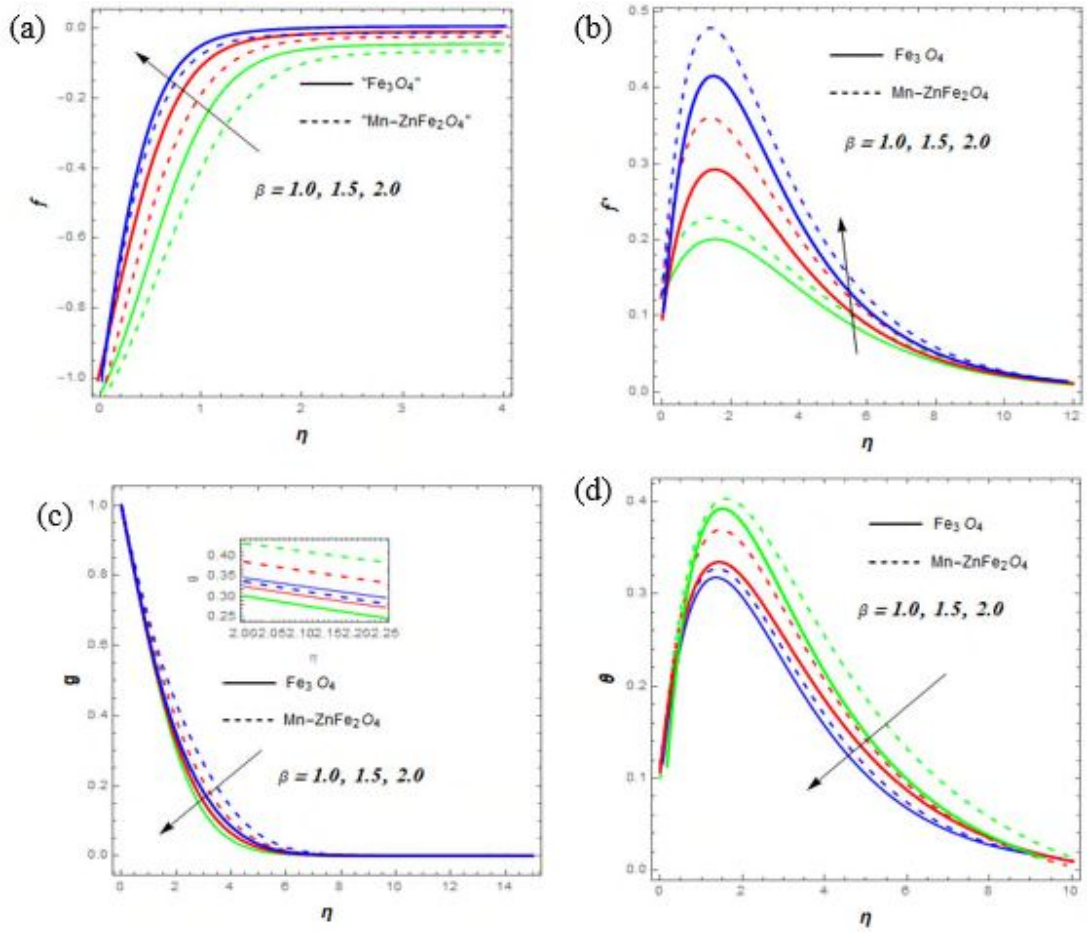

Figure 5: Impact of (β) on (f), (f'), (g) *and* (θ) profiles.

Figure *6* (a, b, c, d). displays the distributions of (f), (f'), (g) and (θ) for different values of volume concentration of the nanoparticle parameter (ϕ_1). Φ_1 relies upon the mass of the magnetic nanoparticles in the base fluid. However, at low magnetic field strength, it is discovered that the mass volume flow of ferromagnetic nanoparticles (Fe_3O_4 and

Mn-$ZnFe_2O_4$) nanofluids reduce with high coefficient of friction. Also, it was observed that the flow rate of ferromagnetic nanoparticles of radial velocity in the far flow direction decreased with increasing fluid friction in response to an increased volume fraction. Moreover, due to increased influences of the intrinsic viscosity and heat flux terms, the bond strength of nanoparticles with a flux size of g(η) reduces by the ferromagnetic material. Consequently, the tangential movement of the spinning disc reduced, and it should be noted that the volumetric concentration in stream did not change significantly (see Figure *6*c). Further, the Adhesion force of ferromagnetic nanoparticles increase with increasing thermal and viscosity effect for ferromagnetic materials. Therefore, the fluid temperature (θ) profile of the rotating disk is dramatically enhanced. This behaviour can be seen in (see Figure *6*d).

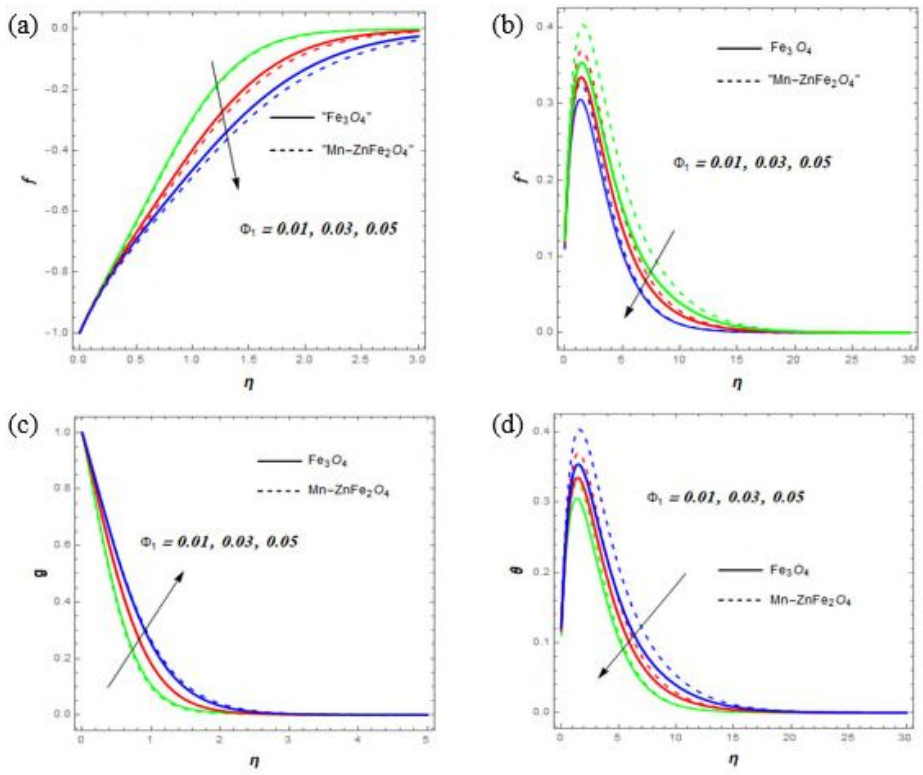

Figure 6: Effect of (β) on (f), (f'), (g) *and* (θ) profiles.

Figure 7(a) displays the distributions of (θ) for different values of Prandtl number parameter (Pr), variable thermal conductivity (ε), and heat generation term (S_T). The connection with both momentum and thermal diffusivities is depicted in the figure. Consequently, the general decrease in the heat exchange field takes place due to the domination of thermal diffusivity, which ensures a strong dissipation of heat from the environment. However, Strong heat diffusion exist in the system, as a result of which a rise in the Prandtl number cause the fluid temperature to be suppressed due to the thinner thermal intrinsic viscosity. An enhancement in the thermodynamic temperature is seen due to the reduction in molecular bond formation between the spinning stretching disk and nanoparticles. Substantially, as the heat source approaches, the chemical bond between the nanoparticles breaks causing more nanoparticle collisions distance from the surface of the disk. Thus, heat transmission of the system from the surface

of the disks has increased significantly. Consequently, the heat generation enhances the heat transmission and improves the conductivity of the considered ferromagnetic nanofluid (see Figure 7(a and b)).

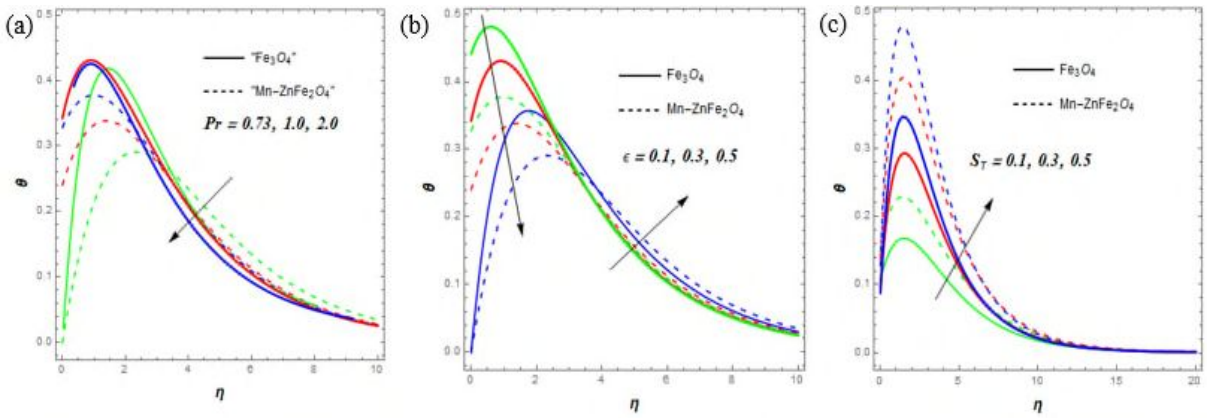

Figure 7: (S_T). (ε), and (Pr) on (θ) profiles.

To ensure the accuracy of the current method, the values of dimensionless radial stress rate, and Nusselt number for the problem were compared to the results of Optimal Homotopy Analysis Method (OHAM) and a strong agreement has been found (see Table 5). Meanwhile, Table 6, and 7 portray the wall boundary friction and heat gradient results of pertinent parameters for the Fe_3O_4 and Mn-$ZnFe_2O_4$-nanofluids. The impact of temperature gradient is well noticeable for the Fe_3O_4 and Mn-$ZnFe_2O_4$-nanofluids at different rates. The physical quantities are either rising or diminishing in response to parameter variation due to shrinkage or expansion of the boundary layer that influence the wall effect.

Table 5**:** Results comparison of GWRM with Analytical Results (OHAM)

		GWRM Results		OHAM Results	
β_1	β_2	$f''(0)$	$\theta'(0)$	$f''(0)$	$\theta'(0)$
0.5	1.0	1.640227	25.994457	1.640212	25.994449
2.0	1.5	1.085158	13.180761	1.085137	13.180745
3.0	2.0	0.844336	9.883323	0.844322	9.883312

Table 6**:** Calculated results of Fe_3O_4-nanoliquid for various wall effect

β	K	δ	ϕ_1	C_f	C_g	Nu
1.5	0.3	0.2	0.1	1.4110470876	-1.4237937881	30.7712960414
2.0				1.5164709650	-1.4298287757	22.7432208157
	0.5			1.5031749301	-1.1891898361	18.2165833451
	0.7			1.4928763982	-1.0715776432	16.3179868420

	0.4		1.5150489780	-1.4293937140	22.8074578697
	0.6		1.5128523882	-1.4287231916	22.9071862957
		0.03	1.6194456289	-1.4633686616	18.6941881579
		0.07	1.5605813960	-1.4437086938	20.8703450518

Table 7**:** Calculated results of Mn-$ZnFe_2O_4$-nanoliquid for different wall effect

Pr	ϵ	S_T	β_1	C_f	C_g	Nu
1.0	0.1	1.0	1.0	1.5912552726	-1.4514173983	14.0425572158
3.0				1.5254516435	-1.4335569973	22.5484182770
	0.3			1.2543289497	-1.4167129996	8.2934312410
	0.5			1.1499220664	-1.4087914807	5.3129097223
		0.5		0.9897931228	-1.3849966723	7.6715795970
		0.7		1.1882657803	-1.4036757633	12.3123545067
			2.0	1.2758338290	-1.4086248031	17.2044138928
			3.0	1.0479046803	-1.3834248738	13.6750429527

5. CONCLUSION

The present work investigated the magnetization characteristics of Fe_3O_4 and Mn-$ZnFe_2O_4$ nanofluids due to a stretchable spinning disk in the existence of variable thermophysical properties using numerical approach. The key outcomes of the present analysis are highlighted as follows:

1. The employed method demonstrates an excellent potential in respect to accuracy and convergence for simulating flow.
2. The ferromagnetic Fe_3O_4 nanofluid shows high thermal conductivity strength than ferromagnetic Mn-$ZnFe_2O_4$ nanoparticles.
3. The magnetic field improved the fluid viscosity that supports the efficiency of industrial machines.
4. The conductive and convective strengths of ferromagnetic nanoparticles were enhanced by mounting values of variable thermal conductivity parameter.
5. The thermal distributions improve as the heat generation term and nanoparticle parameter increase.
6. The flow properties of ferromagnetic Fe_3O_4 nanofluids are more reactive to parameter change than of ferromagnetic Mn-$ZnFe_2O_4$ nanofluids.

Future recommendations: Nanotechnology makes use of unique nanoscale characteristics like paramagnetic to build new technologies and materials. Nevertheless, in the coming years, Ferrofluids might be utilized to transport drugs to parts of the body. However, further extension is therefore needed in this field.

DATA AVAILABILITY STATEMENT

The authors affirm that all the generated data and materials are available within the article.

DISCLOSURE STATEMENT

The authors have no conflict of interest to disclose

REFERENCES

[1] S.A. Sokolsky, A.Y. Solovyova, V.S. Zverev, M. Hess, A. Schmidt, E.A. Elfimova, Journal of Magnetism Magnetic Materials 537 (2021) 168169.
[2] Z. Mehrez, A. El Cafsi, Applied Mathematics Computation 391 (2021) 125634.
[3] M. Kole, S. Khandekar, Journal of Magnetism Magnetic Materials (2021) 168222.
[4] A. Bhandari, Proceedings of the Institution of Mechanical Engineers, Part C:Journal of Mechanical Engineering Science 235 (2021) 2201.
[5] S.E. Hosseinizadeh, S. Majidi, M. Goharkhah, A. Jahangiri, Thermal Science Engineering Progress 25 (2021) 101019.
[6] N. Acharya, Heat Transfer (2021).
[7] T. Von Karman, Transfer ASME 61 (1939) 705.
[8] W. Cochran, Mathematical Proceedings of the Cambridge Philosophical Society, Cambridge University Press, 1934, p. 365-375.
[9] E.R. Benton, Journal of Fluid Mechanics 24 (1966) 781.
[10] S. Shehzad, Z. Abbas, A. Rauf, Z. Abdelmalek, International Communications in Heat and Mass Transfer 120 (2021) 105025.
[11] M. Usman, T. Gul, A. Khan, A. Alsubie, M.Z. Ullah, International Communications in Heat Mass Transfer 127 (2021) 105562.
[12] A. Alhadhrami, C. Vishalakshi, B. Prasanna, B. Sreenivasa, H. Alzahrani, R.P. Gowda, R.N. Kumar, Case Studies in Thermal Engineering (2021) 101483.
[13] S. Saranya, Q.M. Al-Mdallal, Case Studies in Thermal Engineering 25 (2021) 100943.
[14] A. Kotb, H.A. Nasr-El-Din, SPE Journal 26 (2021) 1161.
[15] S. Shehzad, F. Mabood, A. Rauf, M. Izadi, F. Abbasi, Physica Scripta 96 (2021) 035210.
[16] R.N. Kumar, R.P. Gowda, B. Gireesha, B. Prasannakumara, The European Physical Journal Special Topics (2021) 1.
[17] B. Yu, M. Ramzan, S. Riasat, S. Kadry, Y.-M. Chu, M. Malik, Scientific Reports 11 (2021) 1.
[18] G. Sarkar, B. Sahoo, European Journal of Mechanics-B/Fluids 85 (2021) 149.

[19] H. Waqas, U. Farooq, R. Naseem, S. Hussain, M. Alghamdi, Case Studies in Thermal Engineering 26 (2021) 101015.
[20] S. Mandal, G. Shit, Chinese Journal of Physics (2021).
[21] M.G. Reddy, N. Kumar, B. Prasannakumara, N. Rudraswamy, K.G. Kumar, Communications in Theoretical Physics 73 (2021) 045002.
[22] H. Ilyas, I. Ahmad, M.A.Z. Raja, M.B. Tahir, M. Shoaib, International Journal of Hydrogen Energy 46 (2021) 28298.
[23] M.S. Iqbal, I. Mustafa, I. Riaz, A. Ghaffari, W.A. Khan, Heat Transfer 50 (2021) 619.
[24] A.M. Obalalu, F.A. Wahaab, L.L. Adebayo, Journal of Taibah University for Science 14 (2020) 541.
[25] Ajala, Adegbite, Abimbade, Obalalu, International Journal of Applied Mathematics & Statistical Sciences (IJAMSS) 2 (2019).
[26] F.A. Wahaab, L.L. Adebayo, A. Rostami, M. Ganeson, J.Y. Yusuf, Y. Afeez, A.M. Obalalu, A. Abdulraheem, T.L. Oladosu, Indian Journal of Physics (2021) 1.
[27] A.M. Obalalu, Heat Transfer 50 (2021) 7988.
[28] A.M. Obalalu, Journal of the Egyptian Mathematical Society 30 (2022) 1.
[29] M. Abdel-Wahed, M. Akl, AIP Advances 6 (2016) 095308.
[30] M. Uddin, O.A. Bég, N. Amin, Journal of Magnetism Magnetic Materials 368 (2014) 252.
[31] M. Malekan, A. Khosravi, X. Zhao, Applied Thermal Engineering 146 (2019) 146.
[32] A.M. Obalalu, O.A. Ajala, A. Abdulraheem, A.A. Oladimeji, Partial Differential Equations in Applied Mathematics (2021) 100084.
[33] A.M. Obalalu, F.A. Wahaab, L.L. Adebayo, Journal of Taibah University for Science 14 (2020) 541.
[34] X. Zhang, J. Mao, Y. Chen, C. Pan, Z.J.N.F. Xu, Nucl. Fusion 59 (2019) 056018.
[35] M. Khan, T. Salahuddin, S. Stephen, Journal of Molecular Liquids 333 (2021) 115749.
[36] F. Mabood, A. Rauf, B. Prasannakumara, M. Izadi, S. Shehzad, Chinese Journal of Physics 71 (2021) 260.
[37] G. Luo, Z. Yao, Journal of Heat Transfer 143 (2021) 011801.
[38] S.M. Fazeli, V. Kanjirakkad, C. Long, Journal of Engineering for Gas Turbines Power 143 (2021) 071026.
[39] A. Ghaffari, I. Mustafa, T. Muhammad, Y. Altaf, Case Studies in Thermal Engineering 28 (2021) 101370.
[40] M. Nayak, S. Shaw, M.I. Khan, V. Pandey, M. Nazeer, Journal of Materials Research Technology 9 (2020) 7387.
[41] S.M. Upadhya, R.R. Devi, C. Raju, H.M. Ali, Journal of Thermal Analysis Calorimetry 143 (2021) 1973.

[42] M. Alghamdi, Coatings 10 (2020) 86.
[43] A. Akindele, A. Ogunsola, Math. Comput. Sci. 11 (2021) 1486.
[44] C. Zemedu, W. Ibrahim, Mathematical Problems in Engineering 2020 (2020).
[45] J.C. Maxwell, A treatise on electricity and magnetism. Clarendon press, 1873.
[46] F. Jiao, Q. Li, Y. Jiao, Y. He, Journal of Molecular Liquids 328 (2021) 115404.
[47] D. Borin, R. Müller, S. Odenbach, Materials 14 (2021) 1870.
[48] B. Mahanthesh, N.S. Shashikumar, G. Lorenzini, Journal of Thermal Analysis Calorimetry 145 (2021) 3339.
[49] A. Bhandari, Mathematics Computers in Simulation 178 (2020) 290.
[50] A.M. Obalalu, Heat Transfer.
[51] M. Bezaatpour, H.J.A.T.E. Rostamzadeh, 164 (2020) 114462.
[52] A.M. Obalalu, O.A. Ajala, A. Abdulraheem, A.O. Akindele, Partial Differential Equations in Applied Mathematics 4 (2021) 100084.
[53] A. Obalalu, I. Kazeem, A. Abdulrazaq, O. Ajala, A. Oluwaseyi, A. Adeosun, L. Adebayo, F.J.J.S.S.C.M. Wahaab, 14 (2020) 503.
[54] F.A. Wahaab, L.L. Adebayo, A.A. Adekoya, I.G. Hakeem, B. Alqasem, A.M. Obalalu, J. Alloys Compd. 836 (2020) 155272.
[55] F.A. Wahaab, L.L. Adebayo, A.A. Adekoya, J.Y. Yusuf, A.M. Obalalu, A.O. Yusuff, B. Alqasem, Journal of Molecular Liquids 318 (2020) 114378.
[56] M. Abd El-Aziz, A.A. Afify, Entropy 21 (2019) 592.
[57] M.I. Hassan, I.A. Alzarooni, Y. Shatilla, Energy Procedia 75 (2015) 3201.
[58] U. Khan, A. Zaib, A. Ishak, S. Bakar, Case Studies in Thermal Engineering (2021) 101151.
[59] S. Suresh, K. Venkitaraj, P. Selvakumar, M. Chandrasekar, Colloids Surfaces A: Physicochemical Engineering Aspects 388 (2011) 41.

Heat transfer enhancement of magnetized nanofluid flow due to a stretchable rotating disk with variable thermophysical properties effects

Olayemi, Olalekan Adebayo

2022-03-25

Olayemi OA, Obalalu AM, Odetunde CB, Ajala OA. (2022) Heat transfer enhancement of magnetized nanofluid flow due to a stretchable rotating disk with variable thermophysical properties effects. European Physical Journal Plus, Volume 137, Issue 3, March 2022, Article number 393

https://doi.org/10.1140/epjp/s13360-022-02579-w